Solar Energy 218 (2021) 237–250

Contents lists available at ScienceDirect

Solar Energy

journal homepage: www.elsevier.com/locate/solener

Predictive storage strategy for optimal design of hybrid CSP-PV plants with immersion heater

P. Richter [a,*], T. Trimborn [b], L. Aldenhoff [b]

[a] Karlsruhe Institute of Technology (KIT), Steinbuch Centre for Computing, Hermann-von-Helmholtz-Platz 1, 76344 Eggenstein-Leopoldshafen, Germany
[b] RWTH Aachen University, Research Group for Continuous Optimization, Department of Mathematics, Templergraben 55, 52064 Aachen, Germany

ARTICLE INFO

Keywords:
Storage strategy
Model predictive control
Linear programming
Hybrid CSP-PV power plant
Immersion heater

ABSTRACT

A hybrid solar power plant effectively combines the two main advantages of solar power plants: concentrated solar power (CSP) with a cheap thermal storage system and photovoltaic (PV) with cheap electricity production. In a hybrid plant, both systems are coupled with the thermal storage, where an immersion heater can transfer the PV energy into thermal energy. A real-time storage strategy is developed using model predictive control considering the future energy tariff and future weather conditions. The efficiency of the power block is considered as quadratic function in dependency of the bulb temperature. As strategy the optimization problem is formulated as linear program. The methods are tested in a realistic scenario for a hybrid CSP-PV power plant with real weather data and different tariffs. Furthermore, on the basis of the best strategy, the optimal design for CSP, PV and storage size is investigated. In comparison to the state of the art (heuristic) optimization we gain 14 % by using a predictive control strategy in combination with an optimal power plant configuration. We show that the storage strategy not only impacts the achievable plant output but also very strongly the subsystem sizing. It can be seen that the plant configuration is massively influenced by the storage control scheme.

1. Introduction

Extensive usage of conventional energy technologies in the form of fossil fuels has been known to produce negative effects on the environment, resulting in a rapid climate change. To confront and possibly reverse this negative environmental impact there has been a rapid growth in interest in use of renewable energies (Camacho and Berenguel, 2012). Solar energy thus represents one of the greatest opportunities to maximize energy production in a sustainable way.

In this work we regard electrical power production from solar energy via a hybrid power plant with integrated storage system, which bases on concentrated solar power (CSP) and photovoltaic (PV). This type of hybrid plant takes advantages of both concentrated solar thermal and photovoltaic plants: cheap solar electricity and an effective thermal storage which is coupled with the PV plant via an immersion heater.

For a cost-efficient operation of this hybrid power plant a real-time storage strategy should be used, which uses the forecast of weather conditions. Furthermore, it is important to investigate how the storage strategy has an influence on the optimal design for CSP, PV and storage size as part of the layout optimization.

1.1. State of the art

In literature, several approaches are proposed for the operation of the thermal storage. The focus of the strategies is usually on maximization of plant revenue or minimization of plant costs. The strategy approaches can more or less be divided into two different categories: Reactive control methods which decide for a control mode, and mathematical optimization using model predictive control for Pontryagin's maximum principle.

Guédez et al. (2014) consider the integration of thermal energy storage system from two perspectives that take into account the market role of concentrating solar power plants. Thus, they differentiate between the continuous power production where the goal is to produce electricity during all 24 h of the day and the peaking power production where the goal is to shift power production to times when it is needed the most (i.e. usually when the market prices of electricity are higher). The storage strategy bases on a an instant-dispatch and peaking operation. Casella et al. (2014) focus on optimal control of the plant, while optimizing each month of the operation. They demonstrate the influence a storage size can have on the overall performance, as it determines the quantity of production that can be deferred. Cirocco et al. (2015) consider the storage system with an infinite capacity and only three

* Corresponding author.
E-mail address: pascal.richter@kit.edu (P. Richter).

https://doi.org/10.1016/j.solener.2020.11.005
Received 18 August 2020; Received in revised form 19 October 2020; Accepted 1 November 2020
Available online 13 March 2021

Nomenclature

P_{th}^{sb}	Thermal power of the concentrated solar block [MW_{th}]
$P_{th}^{sb,pb}$	Thermal power sent from concentrated solar block to the power block [MW_{th}]
$P_{th}^{sb,st}$	Thermal power sent from concentrated solar block to the storage [MW_{th}]
$P_{th}^{st,pb}$	Thermal power sent from storage to the power block [MW_{th}]
P_{th}^{pb}	Thermal power of the power block [MW_{th}]
$P_{el}^{pb,grid}$	Electric power from the power block directed to the grid [MW_{el}]
$P_{th}^{sb,excess}$	Thermal power excess directed out of the CSP system [MW_{th}]
P_{el}^{pv}	Electric power of the photovoltaic modules [MW_{el}]
$P_{el}^{pv,st}$	Electric power from photovoltaic modules directed to the thermal storage [MW_{el}]
$P_{el,DC}^{pv,grid}$	Electric DC power from photovoltaic modules directed to the grid [MW_{el}]
$P_{el}^{pv,grid}$	Electric AC power from photovoltaic modules directed to the grid [MW_{el}]
$P_{th}^{pv,excess}$	Potential electrical access power of the PV system, not produced [MW_{el}]
Q_{th}^{st}	Stored thermal energy in storage [MW_{th} h]
I_{DNI}	Solar direct normal irradiance [W/m^2]
I_{GHI}	Global horizontal irradiance [W/m^2]
I_{DHI}	Diffuse horizontal irradiance [W/m^2]
$T_{ambient}$	Ambient temperature [°C]
T_{bulb}	Dry or wet bulb temperature [°C]
$p_{ambient}$	Ambient air pressure [mbar]
v_{wind}	Wind speed [m/s]
η_{st_in}	Storage charging efficiency [%]
η_{st_out}	Storage discharging efficiency [%]
η_{pb}	Efficiency in the power block for conversion of thermal power to electric power [%]
$\eta_{immersion}$	Efficiency for conversion of PV electric DC power to thermal power [%]
$\eta_{inverter}$	Efficiency for DC to AC electric power conversion [%]

distinct control modes of operation. Wittmann et al. (2011) present the optimization of a price-driven operation strategy using dynamic programming, while taking into account the physical (e.g. storage capacity) and technical (e.g. maximum overload situations) constraints, as well as solar forecasts. The strategy is mostly determined only by the direct solar irradiation forecast, while price fluctuations in the market are not taken into account.

Usaola (2012) focus on maximizing the plant revenue, while taking into account daily electricity prices. They model the strategy as a mixed-integer problem and demonstrate the one-day and two-day strategy optimization. Camacho et al. (2014) and Camacho and Gallego (2015) introduce the optimal scheduling for energy production using model predictive control. However, they do not consider tariffs for energy production in their work, and focus on the optimization for determining the amount of energy that needs to be released from the concentrated solar block. Cirocco et al. (2016) consider the storage system with an infinite capacity and use Pontraygin's maximum principle to determine the optimal strategy for maximizing the revenue. Vasallo and Bravo (2016) introduce a model predictive control with mixed-integer programming for optimal generation scheduling in CSP plants, and consider the market in their model.

With regards to the hybrid CSP-PV plant, to the knowledge of the author the way of storing PV power in the thermal storage of the CSP plants has not yet been studied. There are some works with regard to the usage of batteries for storing the power produced by PV plant (Dominio, 2014). Zhai et al. (2018) also use batteries for the PV plant, where they optimize the hybrid CSP-PV plant design by using the genetic algorithm. The plant design is optimized with respect to the PV-capacity, PV battery capacity and CSP thermal storage capacity, while taking into account a fixed CSP capacity and plant costs.

In this paper we model a hybrid CSP-PV plant, where the PV plant supplementary can use an immersion heater to thermally store energy. To our knowledge this hybrid CSP-PV plant with shared thermal storage has not been investigated so far in literature. For finding an optimal storage strategy we follow the ideas of model predictive control using mixed-integer programming. Thus, we will adapt the works of Vasallo and Bravo (2016) for the extended model with a shared thermal storage. Beside the model extension, we will improve the model by considering the efficiency of the power block as non-linear function. In such a way the model is more realistic as it considers the influence of different power loads and bulb temperatures for the power production, which was neglected so far.

1.2. Outline

The paper is structured as follows: Section 2 will introduce the hybrid solar power plant and presents a mathematical model for all components. In Section 3 two different storage strategies are developed. While the first one is just a simple reactive control method for comparison reasons, the other one bases on model predictive control using mixed-integer programming. Section 4 validates the different strategies. For a realistic test scenario with real weather data and different tariffs the influence of the considered forecast time and the computational time is investigated. Furthermore, the optimal design of a hybrid CSP-PV power plant with regard to the capacities for CSP, PV and thermal storage optimal design is examined. The final conclusions are drawn in Section 5.

2. Modeling a hybrid CSP-PV power plant

A hybrid CSP-PV solar power plant effectively combines the benefits of a cheap storage system and a cheap electricity production. Both systems are coupled with the thermal storage, where an immersion heater can transfer the PV energy into thermal energy, see Fig. 1.

The whole power plant can be sub-divided into four blocks: the photovoltaic block for producing electric power, the concentrated solar block (e.g. a parabolic trough collector field) for producing thermal power, the storage block for storing thermal power, and the power block for conversion from thermal to electric power. The blocks are connected by the power flows between them, see Fig. 2. In the following, all four models of the hybrid solar power plant are developed.

2.1. Photovoltaic model

Photovoltaic systems represent the most common way of producing electricity from solar energy. While concentrated solar power plants convert solar irradiance to thermal power, photovoltaic power plants directly convert the solar irradiation into electric direct current (DC), see Parida et al. (2011). Beside feeding energy to the grid, for the hybrid power plant there exists also the option of charging the thermal storage of the CSP plant by operating an immersion heater with DC power, which heats up the molten salt from the cold storage tank and stores it

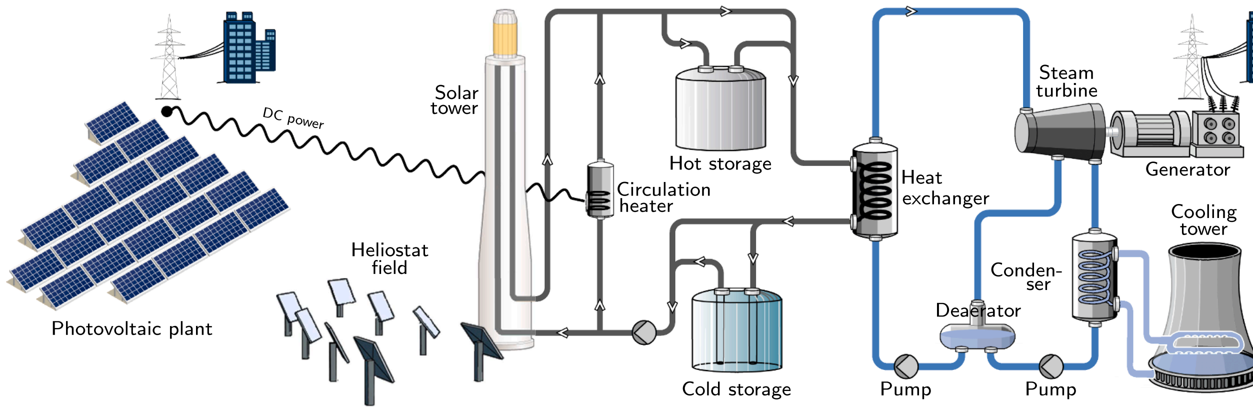

Fig. 1. Overview of a hybrid CSP-PV power plant with thermal energy storage using a central receiver system. The PV component converts the solar power into electric DC power. The electric DC power is converted into electric AC power and sent to the grid, or directly sent to the immersion heater to heat up molten salt and store it into the thermal storage system as thermal energy.

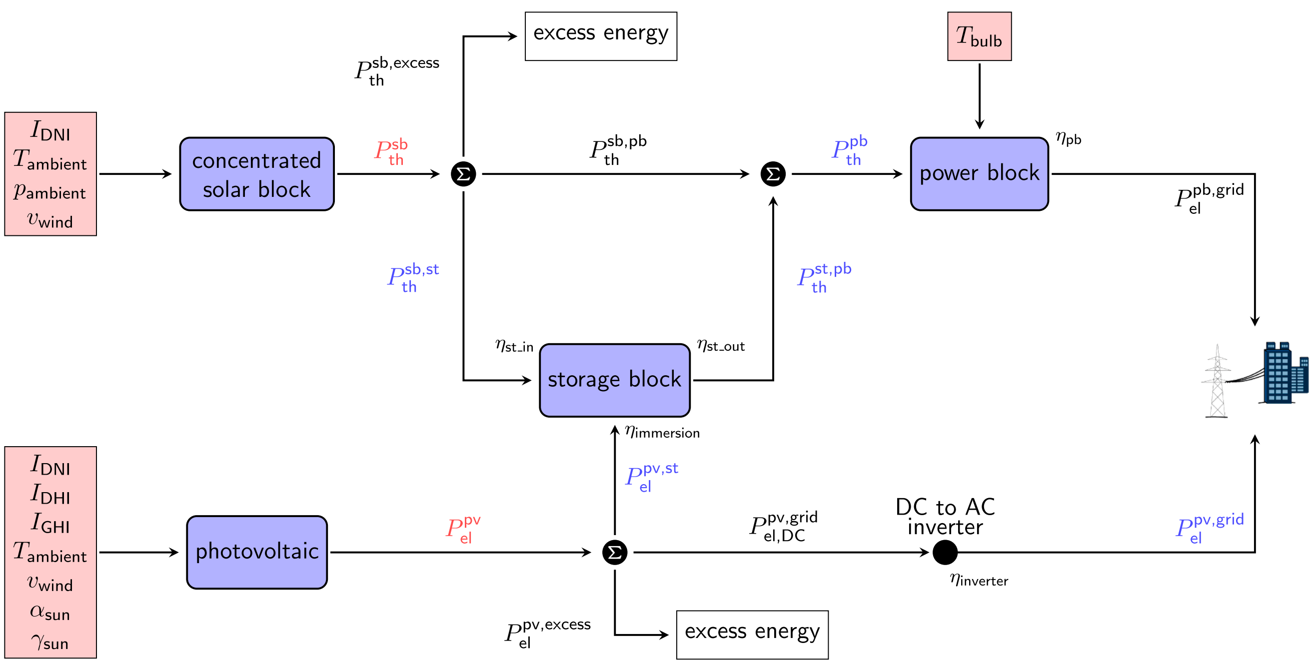

Fig. 2. Model of a hybrid CSP-PV power plant, containing the photovoltaic block, concentrated solar block, power block, and storage block. The red boxes show the time-dependent input parameters for each single sub-model. The blocks are connected by the power flows between them. The excess energy branch of the concentrated solar block represents the energy that is discarded from the system for the situations when part of the solar field needs to be defocused. The excess energy branch of the photovoltaic block represents the energy that is discarded from the system for the situations when the PV power cannot be stored, and cannot be added to the grid (due to some grid limitations). The decision parameters are marked in blue, while the given parameters at each instance of time are marked in red. The in black marked parameters are given as a consequence of the other parameters.

into the hot storage tank as thermal energy.

Thus, the electric power produced by the photovoltaic plant is sent to the grid $P_{\text{el,DC}}^{\text{pv,grid}}$, or it is charged as thermal power $P_{\text{el}}^{\text{pv,st}}$ in the thermal storage system of the CSP plant, such that it holds:

$$P_{\text{el,DC}}^{\text{pv,grid}}(t) + P_{\text{el}}^{\text{pv,st}}(t) \leqslant P_{\text{el}}^{\text{pv}}(t). \tag{1}$$

The excess energy represents the energy that is discarded from the system for the situations when the PV power cannot be stored and cannot be added to the grid,

$$P_{\text{el}}^{\text{pv,excess}}(t) = P_{\text{el}}^{\text{pv}}(t) - P_{\text{el,DC}}^{\text{pv,grid}}(t) - P_{\text{el}}^{\text{pv,st}}(t). \tag{2}$$

As for the grid alternating current (AC) is required, an inverter subsystem (with an efficiency of η_{inverter}) converts from DC to AC, such that the feed into the grid is given by

$$P_{\text{el}}^{\text{pv,grid}}(t) = \eta_{\text{inverter}} \cdot P_{\text{el,DC}}^{\text{pv,grid}}(t). \tag{3}$$

The electrical power of a PV cell can be computed by Zhai et al. (2018),

$$P_{\text{el}}^{\text{pv}}(t) = A_{\text{pv}} \cdot I(t) \cdot \eta_{\text{pv}}(t) \cdot \eta_{\text{cleanliness}}, \tag{4}$$

with A_{pv} representing the panel area, I the total solar irradiation on the panels, and η_{pv} the PV panel efficiency. The cleanliness of the PV panels $\eta_{\text{cleanliness}}$ accounts for the degree of soiling, wiring losses, shading, snow cover, aging, and other secondary losses. The efficiency of a PV panel is represented as

$$\eta_{\text{pv}}(t) := \eta_{\text{pv,nominal}} \cdot (1 + \gamma_T \cdot (T_{\text{pv}}(t) - T_{\text{std}})), \tag{5}$$

with $\eta_{\text{pv,nominal}}$ as nominal PV panel efficiency, γ_T as temperature factor, and T_{std} as temperature under standard conditions. The operating temperature T_{pv} is modeled according to Zhai et al. (2018),

$$T_{\text{pv}}\left(t\right)=T_{\text{ambient}}\left(t\right)+\left(T_{\text{nominal}}-T_{\text{ambient,nominal}}\right)\cdot\frac{I(t)}{I_{\text{nominal}}}\cdot\frac{U_{\text{nominal}}}{U(t)}\cdot\left(1-\frac{\eta_{\text{pv}}(t)}{\tau_{\text{abs}}}\right), \tag{6}$$

where under nominal conditions T_{nominal} represents the operating cell temperature, $T_{\text{ambient,nominal}}$ the ambient temperature, I_{nominal} the solar irradiation, U_{nominal} the rated heat transfer factor, and τ_{abs} the transmittance absorption coefficient. Below in Table 1 these parameters are set to their default value given by Zhai et al. (2018). Furthermore, $T_{\text{ambient}}(t)$ is the actual ambient temperature and $I(t)$ the actual solar irradiation. The fluid velocity $U(t)$ leading to heat transfer is estimated as

$$U(t) := 5.7\,[\text{m/sec}]+3.8\cdot v_{\text{wind}}(t), \tag{7}$$

with $v_{\text{wind}}(t)$ as the wind speed.

The total solar irradiation $I(t)$ on the panels from Eq. (4) depends on the tracking system of the photovoltaic system. For large plants usually a horizontal single-axis tracker is used that rotates around the horizontal axis for tracking the sun. Altogether, the total solar irradiation $I(t)$ is given by Masters (2013),

$$I\left(t\right) := I_{\text{DNI}}\left(t\right)\cdot\cos\left(\theta_{\text{sun}}\left(t\right)\right)+I_{\text{DHI}}\left(t\right)\left(\frac{1}{2}+\frac{\sin(\alpha_{\text{sun}}(t))}{2\cos(\theta_{\text{sun}}(t))}\right)+\eta_{\text{ground}}\cdot I_{\text{GHI}}\left(t\right)\left(\frac{1}{2}-\frac{\sin(\alpha_{\text{sun}}(t))}{2\cos(\theta_{\text{sun}}(t))}\right), \tag{8}$$

where η_{ground} is the ground reflectance. With α_{sun} as the solar altitude, γ_{sun} as solar azimuth, and $\gamma_{\text{collector}}$ as collector azimuth angle, the incidence angle θ_{sun} between collector and sun is given by

$$\cos\left(\theta_{\text{sun}}\left(t\right)\right) = \sqrt{1-(\cos\alpha_{\text{sun}}(t)\cdot\sin(\gamma_{\text{sun}}(t)-\gamma_{\text{collector}}))^2}. \tag{9}$$

The solar direct normal irradiation I_{DNI}, diffuse horizontal irradiation I_{DHI}, and global horizontal irradiation I_{GHI} are given by meteorological data.

The size of a PV plant is usually denoted by the peak electrical power $P_{\text{el}}^{\text{pv-peak}}$, which corresponds to the electrical power (4) of a PV cell under nominal conditions,

$$P_{\text{el}}^{\text{pv-peak}} = A_{\text{pv}}\cdot I_{\text{nominal}}\cdot\eta_{\text{pv,nominal}}\cdot\eta_{\text{cleanliness}}. \tag{10}$$

In a case study in Section 4.2 an optimal nominal power is found (which correlates to an optimal PV area A_{pv}) for a hybrid CSP-PV plant.

2.2. Concentrated solar block model

As heat source of the concentrated solar block a central receiver system is used. The concentrated solar block converts direct normal irradiation to thermal power in the receiver unit by heating up the heat transfer fluid. It is assumed that the solar thermal system always delivers the nominal temperature, for which the storage and turbine are designed for. Altogether, the produced thermal power in the concentrated solar block $P_{\text{th}}^{\text{sb}}$ can be described by a function

$$P_{\text{th}}^{\text{sb}} := P_{\text{th}}^{\text{sb}}(\alpha_{\text{sun}}(t),\gamma_{\text{sun}}(t),I_{\text{DNI}}(t),T_{\text{ambient}}(t),p_{\text{ambient}}(t),v_{\text{wind}}(t)), \tag{11}$$

with solar altitude α_{sun}, solar azimuth γ_{sun}, and solar direct normal irradiation I_{DNI} for the solar field. For the thermal receiver device we need the values for the ambient temperature T_{ambient}, ambient air pressure p_{ambient} and wind velocity v_{wind}. The actual function depends on the heliostat field layout and the receiver layout. For the calculation of thermal output power in this work, the *STRAL* raytracer tool was used, see Ahlbrink et al. (2012). The heat transfer fluid is transferred from the receiver either directly to the power block via a heat exchanger or to the storage system, see Fig. 1.

The size of a solar field is usually denoted by the nominal thermal power $P_{\text{th}}^{\text{sb-nominal}}$, which corresponds to the thermal power (11) under nominal conditions. In a case study in Section 4.2 this parameter (which somehow correlates to the mirror area) is optimized for a hybrid CSP-PV plant.

The thermal power produced by the concentrated solar block is sent to the power block $P_{\text{th}}^{\text{sb,pb}}$, or used for storing as thermal power $P_{\text{th}}^{\text{sb,st}}$ in the storage system, such that it holds

$$P_{\text{th}}^{\text{sb,pb}}(t)+P_{\text{th}}^{\text{sb,st}}(t)\leqslant P_{\text{th}}^{\text{sb}}(t). \tag{12}$$

The excess energy represents the energy that is discarded from the system for the situations when the thermal power cannot be stored and cannot be added to the power block,

$$P_{\text{th}}^{\text{sb,excess}}(t) = P_{\text{th}}^{\text{sb}}(t)-P_{\text{th}}^{\text{sb,pb}}(t)-P_{\text{th}}^{\text{sb,st}}(t). \tag{13}$$

2.3. Storage model

The amount of currently stored thermal energy is defined as $Q_{\text{th}}^{\text{st}}$. The stored energy changes by charging with the incoming power from the concentrated solar block $P_{\text{th}}^{\text{sb,st}}$ or photovoltaic plant $P_{\text{th}}^{\text{pv,st}}$. Similarly, the stored energy decreases by discharging, if thermal power is send to the power block via $P_{\text{th}}^{\text{st,pb}}$. The power losses for charging and discharging are considered by the efficiencies $\eta_{\text{st\_in}}$ and $\eta_{\text{st\_out}}$, see Usaola (2012). To consider the temperature-driven heat loss from the storage tank to the environment, we simplified assume an hourly loss $\xi_{\text{st\_loss}}$ as a percentage of the stored heat. Altogether, within a time step the changes of the storage fill level of the thermal energy is given by

$$\frac{dQ_{\text{th}}^{\text{st}}}{dt} = \eta_{\text{st\_in}}\cdot P_{\text{th}}^{\text{sb,st}}\left(t\right)+\eta_{\text{immersion}}\cdot P_{\text{el}}^{\text{pv,st}}\left(t\right)-\eta_{\text{st\_out}}^{-1}\cdot P_{\text{th}}^{\text{st,pb}}\left(t\right)-\xi_{\text{st\_loss}}\cdot Q_{\text{th}}^{\text{st}}\left(t\right). \tag{14}$$

As the storage is limited by its maximum capacity $Q_{\text{th}}^{\text{st-max}}$ for storing thermal energy, it always must hold

$$0\leqslant Q_{\text{th}}^{\text{st}}(t)\leqslant Q_{\text{th}}^{\text{st-max}}. \tag{15}$$

Furthermore, we must ensure that the strategy just uses the additional resources, such that the fill level of the thermal storage is at the end at least as large as at the begin (Cirocco et al., 2015),

$$Q_{\text{th}}^{\text{st}}(t_{\text{end}})\geqslant Q_{\text{th}}^{\text{st}}(t_0), \tag{16}$$

with an initial fill level at t_0 as given boundary condition. We choose

$$Q_{\text{th}}^{\text{st}}(t_0) := 0, \tag{17}$$

such that the constraint (16) is implicitly fulfilled as long as (15) holds.

Table 1
Parameter settings for the realistic scenario of a hybrid CSP-PV power plant in the MENA region. The needed parameters for the PV model were taken from Zhai et al. (2018, 2013). The four indicated parameters in the last column are optimized in Section 4.2.

Parameter		Value	Optimization
	Site of hybrid CSP-PV plant	Casablanca, 33.58° N, 7.62° W	
P_{el}^{max}	Max power to grid of hybrid CSP-PV plant	200 MW_{el}	
$P_{el}^{pv-peak}$	Photovoltaic peak power	400 MW_{el}	•
$\eta_{cleanliness}$	Cleanliness of the PV panels	80 %	
$\eta_{immersion}$	Efficiency for conversion from DC to thermal power with immersion heater 97.5 %		
$\eta_{inverter}$	Efficiency for conversion from DC to AC	97.8 %	
$\eta_{pv,nominal}$	Nominal PV panel efficiency	14.9 %	
γ_T	Temperature coefficient of power	−0.41 %/°C	
T_{std}	Temperature under standard conditions	25 °C	
$T_{nominal}$	Nominal operating cell temperature	46 °C	
$T_{ambient,nominal}$	Ambient temperature for nominal operating cell temperature 20 °C		
$I_{nominal}$	Nominal global solar irradiation	800 W/m^2	
$U_{nominal}$	Nominal rated heat transfer factor	9.5 m/s	
τ_{abs}	Nominal transmittance absorption coefficient	80 %	
$\gamma_{collector}$	Collector southern azimuth angle	0°	
η_{ground}	Ground reflectance	20%	
$P_{th}^{sb-nominal}$	Concentrated solar block nominal thermal power	150 MW_{th}	•
η_{st-in}	Storage charging efficiency	97 %	
η_{st-out}	Storage discharging efficiency	97 %	
$\xi_{st-loss}$	Storage heat loss factor	0.05 %/h	
Q_{th}^{st-max}	Storage maximum capacity	1200 $MW_{th}h$	•
P_{th}^{pb-min}	Power block minimum power for operation	10 MW_{th}	
P_{th}^{pb-max}	Power block maximum power for operation	125 MW_{th}	•
η_{pb}	Power block efficiency load curve	c_0 : 39.99 c_1 : 0.09991 K^{-1} c_2 : −0.00378 K^{-2}	
η_{pb}^{min}	Minimum power block efficiency	37.9366 %	
π	Tariff for energy production	6:00 – 10:59: 100 €/$MW_{el}h$ 11:00 – 17:59: 50 €/$MW_{el}h$ 18:00 – 19:59: 100 €/$MW_{el}h$ 20:00 – 5:59: 145 €/$MW_{el}h$	
π^{min}	Minimum tariff for energy production	50 €/$MW_{el}h$	

2.4. Power block model

The power block consists of the heat exchanger (i.e. steam generator), steam turbine, generator and the cooling system, see Fig. 1. The thermal power arrives at the heat exchanger as heated molten salt directly from the concentrated solar block $P_{th}^{sb,pb}$ or from the thermal storage $P_{th}^{st,pb}$,

$$P_{th}^{pb}(t) = P_{th}^{sb,pb}(t) + P_{th}^{st,pb}(t). \tag{18}$$

As the turbine can just operate within a defined range, the incoming thermal power is limited by

$$P_{th}^{pb-min} \leqslant P_{th}^{pb}(t) \leqslant P_{th}^{pb-max}. \tag{19}$$

In the power block unit the incoming thermal power P_{th}^{pb} is converted into electric power,

$$P_{el}^{pb,grid}(t) = \eta_{pb}(T_{bulb}(t)) \cdot P_{th}^{pb}(t), \tag{20}$$

where the conversion function η_{pb} describes the power block efficiency. In reality the turbine efficiency also strongly depends on the thermal power flow $P_{th}^{pb}(t)$. But as later in Section 3.2 we want to describe the scheduler as linear optimization problem, it is required that we neglect the dependency from $P_{th}^{pb}(t)$. Therefore we model the power block efficiency η_{pb} as a quadratic polynomial from the wet or dry (depends on the cooling system of the power block) bulb temperature T_{bulb}:

$$\eta_{pb}(T_{bulb}) = c_0 + c_1 \cdot T_{bulb} + c_2 \cdot T_{bulb}^2. \tag{21}$$

In Fig. 3 the power block efficiency η_{pb} is shown, using fitted data from of a 100 MW turbine. The underlying coefficients are given in Table 1 in Section 4.

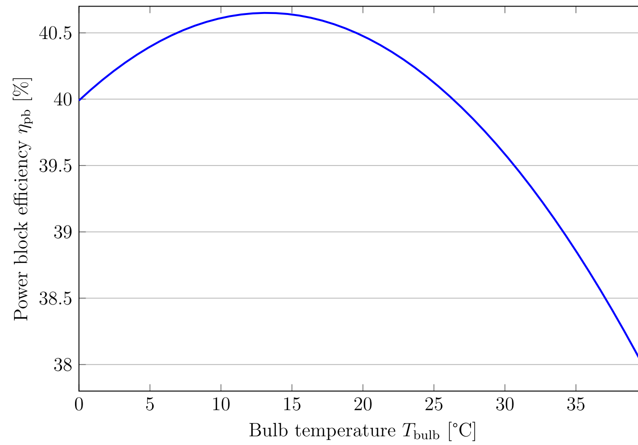

Fig. 3. Power block efficiency η_{pb} (in %) for converting thermal power into electrical power. Characteristic Diagram of a power conversion unit according to simulated data. The efficiency decreases for higher bulb temperatures.

2.5. Economic model

The power plant is controlled over some finite time period $[t_0, t_{end}]$. During the whole period we need to ensure that the electrical power of the hybrid power plant which can be fed into the grid is limited by P_{el}^{max}. Thus, for the summed electrical power from the power block $P_{el}^{pb,grid}$ and the PV modules $P_{el}^{pv,grid}$, it must always hold that

$$0 \leqslant P_{el}^{pb,grid}(t) + P_{el}^{pv,grid}(t) \leqslant P_{el}^{max}, \quad \forall t \in [t_0, t_{end}]. \tag{22}$$

In the following we regard a complete year, thus $t_0 = 0$ [hours], and $t_{end} = 8760$ [hours]. The quality of a storage strategy is in general measured by the annual revenue (in monetary units), which is defined as

$$R_{annual} = \int_{t_0}^{t_{end}} \pi(t) \cdot \left(P_{el}^{pb,grid}(t) + P_{el}^{pv,grid}(t)\right) dt \tag{23}$$

for a full year from t_0 to t_{end}, with $\pi(t)$ as time-dependent tariff for the energy production. The time interval is discretized in equidistant time steps of the length Δt. The step size directly depends on the electricity market which define the tariff $\pi(t)$, and depends on the resolution of the meteorological data[1] used by the photovoltaic and CSP models. Thus, for the discrete time steps $t_i = t_0 + i\cdot\Delta t$ for $i = 0\ldots N$ with length $\Delta t = \frac{t_{\text{end}}-t_0}{N+1}$ the continuously described annual revenue is approximated by

$$R_{\text{annual}} \approx \sum_{i=0}^{N} \pi\left(t_i\right)\cdot\Delta t\cdot\left(P_{\text{el}}^{\text{pb,grid}}(t_i) + P_{\text{el}}^{\text{pv,grid}}(t_i)\right) + \pi^{\min}\cdot\eta_{\text{pb}}^{\min}\cdot Q_{\text{th}}^{\text{st}}\left(t_N\right) \tag{24}$$

An additional term has been added to the original revenue expression to reward the supplementary thermal energy in the storage at the end of the time interval. We choose

$$\begin{aligned} \pi^{\min} &:= \min_{t\in[t_0,t_{\text{end}}]} \pi\left(t\right), \\ \eta_{\text{pb}}^{\min} &:= \min_{T_{\text{bulb}}\in[0,40]} \eta_{\text{pb}}(T_{\text{bulb}}) \end{aligned} \tag{25}$$

as lowest tariff and lowest power block efficiency, such that it is more attractive to produce energy during the time interval instead of storing supplementary energy in the storage.

3. Storage strategy

A storage strategy is needed to find the power flows between the concentrated solar block, storage, photovoltaic modules and the grid. We want to maximize the discretized annual revenue R_{annual} (24) of the power plant for the time period $t \in [t_0, t_{\text{end}}]$. In the following we present a non-predictive heuristic strategy, and a model predictive control strategy using exact optimization as linear program (LP) formulation.

3.1. Non-predictive heuristic strategy

The non-predictive heuristic strategy reduces the usage of the storage by producing electric energy directly when it is available. With reference to the storage strategy introduced in Cirocco et al. (2016), we extend the strategy by incorporating the PV power. At each instance of time t_i, the tariff $\pi(t_i)$, the produced power $P_{\text{th}}^{\text{sb}}(t_i)$ and $P_{\text{el}}^{\text{pv}}(t_i)$, and the current fill level of the storage $Q_{\text{th}}^{\text{st}}(t_i)$ are given, while the control strategy needs to decide the internal power flows between the concentrated solar block, storage, photovoltaic modules and the grid: $P_{\text{th}}^{\text{sb,st}}(t_i)$, $P_{\text{th}}^{\text{sb,pb}}(t_i)$, $P_{\text{th}}^{\text{st,pb}}(t_i)$, $P_{\text{th}}^{\text{pb}}(t_i)$, $P_{\text{el}}^{\text{pb,grid}}(t_i)$, $P_{\text{el}}^{\text{pv,st}}(t_i)$, $P_{\text{el,DC}}^{\text{pv,grid}}(t_i)$, $P_{\text{el}}^{\text{pv,grid}}(t_i)$.

The following strategy bases on the assumption that the PV power is cheaper than the power from the CSP plant. Therefore, with highest priority the PV power is directed to the grid, while for the CSP plant the *generate* and *surplus* mode is applied.

1. The PV power which is fed into the grid is given by

$$P_{\text{el}}^{\text{pv,grid}}(t_i) = \min\left(P_{\text{el}}^{\max},\ \eta_{\text{inverter}}\cdot P_{\text{el}}^{\text{pv}}(t_i)\right), \tag{26}$$

with

$$P_{\text{el,DC}}^{\text{pv,grid}}\left(t_i\right) = \eta_{\text{inverter}}^{-1}\cdot P_{\text{el}}^{\text{pv,grid}}\left(t_i\right). \tag{27}$$

The remaining power $P_{\text{el}}^{\text{pv}}(t_i) - P_{\text{el,DC}}^{\text{pv,grid}}(t_i)$ is used to charge the thermal storage,

$$P_{\text{el}}^{\text{pv,st}}\left(t_i\right) = \min\left(P_{\text{el}}^{\text{pv}}\left(t_i\right) - P_{\text{el,DC}}^{\text{pv,grid}}\left(t_i\right),\ \eta_{\text{immersion}}^{-1}\cdot\frac{1}{\Delta t}\cdot\left(Q_{\text{th}}^{\text{st\_max}} - \left(1-\xi_{\text{st\_loss}}\cdot\Delta t\right)\cdot Q_{\text{th}}^{\text{st}}(t_i)\right)\right). \tag{28}$$

The surplus PV power $P_{\text{el}}^{\text{pv}}$ that cannot be directed to the grid $P_{\text{el,DC}}^{\text{pv,grid}}$ or stored $P_{\text{el}}^{\text{pv,st}}$ is discarded from the system,

$$P_{\text{el}}^{\text{pv,excess}}\left(t_i\right) = P_{\text{el}}^{\text{pv}}\left(t_i\right) - P_{\text{el,DC}}^{\text{pv,grid}}\left(t_i\right) - P_{\text{el}}^{\text{pv,st}}\left(t_i\right). \tag{29}$$

2. For the CSP part at maximum an electric power of $P_{\text{el}}^{\text{pb,grid}}(t_i) \overset{!}{\leqslant} P_{\text{el}}^{\max} - P_{\text{el}}^{\text{pv,grid}}(t_i)$ can be generated in the power plant, to not violate the grid limitations (22). For the given bulb temperature $T_{\text{bulb}}(t_i)$, this corresponds to a maximum possible thermal power in the power block of

$$P_{\text{th}}^{\text{pb,max\_possible}}\left(t_i\right) = \min\left(\left(P_{\text{el}}^{\max} - P_{\text{el}}^{\text{pv,grid}}(t_i)\right)\cdot\eta_{\text{pb}}^{-1}(T_{\text{bulb}}(t_i)),\ P_{\text{th}}^{\text{pb,max}}\right). \tag{30}$$

With this value $P_{\text{th}}^{\text{pb,max\_possible}}(t_i)$ the thermal power from the concentrated solar block to the power block can be determined,

$$P_{\text{th}}^{\text{sb,pb}}\left(t_i\right) = \min\left(P_{\text{th}}^{\text{sb}}\left(t_i\right),\ P_{\text{th}}^{\text{pb,max\_possible}}\left(t_i\right)\right). \tag{31}$$

Any additional power that can be processed by the power block is drawn from the storage (generate mode):

$$\begin{aligned} P_{\text{th}}^{\text{st,pb}}\left(t_i\right) = \min\Bigg(&\eta_{\text{st\_out}}\cdot\left(\frac{1}{\Delta t}\cdot\left(1-\xi_{\text{st\_loss}}\cdot\Delta t\right)\cdot Q_{\text{th}}^{\text{st}}\left(t_i\right)\right. \\ &\left.+\,\eta_{\text{immersion}}\cdot P_{\text{el}}^{\text{pv,st}}\left(t_i\right)\right), P_{\text{th}}^{\text{pb,max\_possible}}\left(t_i\right) - P_{\text{th}}^{\text{sb,pb}}\left(t_i\right)\Bigg). \end{aligned} \tag{32}$$

Then, the total thermal power which is send to the power block is given by the sum

$$P_{\text{th}}^{\text{pb}}\left(t_i\right) = P_{\text{th}}^{\text{sb,pb}}\left(t_i\right) + P_{\text{th}}^{\text{st,pb}}\left(t_i\right), \tag{33}$$

which results in an electric power of

$$P_{\text{el}}^{\text{pb,grid}}\left(t_i\right) = \eta_{\text{pb}}(T_{\text{bulb}}(t_i))\cdot P_{\text{th}}^{\text{pb}}\left(t_i\right). \tag{34}$$

[1] Meteorological data is usually given in 15 min or one hour steps.

Remaining power from the concentrated solar block $P_{th}^{sb}(t_i) - P_{th}^{sb,pb}(t_i)$ is used to charge the thermal storage (surplus mode),

$$P_{th}^{sb,st}(t_i) = \min\Big(P_{th}^{sb}(t_i) - P_{th}^{sb,pb}(t_i),\ \eta_{st\_in}^{-1}\cdot\Big(\frac{1}{\Delta t}\big(Q_{th}^{st\_max} - (1-\xi_{st\_loss}\cdot\Delta t)\cdot Q_{th}^{st}(t_i)\big) - \eta_{immersion}\cdot P_{el}^{pv,st}(t_i) + \eta_{st\_out}^{-1}\cdot P_{th}^{st,pb}(t_i)\Big)\Big). \tag{35}$$

The surplus power from the concentrated solar block P_{th}^{sb} that cannot be directed to the power block $P_{th}^{sb,pb}$ or stored $P_{th}^{sb,st}$ is discarded from the system (13),

$$P_{th}^{sb,excess}(t_i) = P_{th}^{sb}(t_i) - P_{th}^{sb,pb}(t_i) - P_{th}^{sb,st}(t_i). \tag{36}$$

Within each time step, the storage level changes due to loading from the concentrated solar block and photovoltaic modules or due to unloading for the power block. Furthermore we need to consider the thermal losses, see (14), such that,

$$\begin{aligned} Q_{th}^{st}(t_{i+1}) =& Q_{th}^{st}(t_i) + \Delta t\cdot\Big(\eta_{st\_in}\cdot P_{th}^{sb,st}(t_i) + \eta_{immersion}\cdot P_{el}^{pv,st}(t_i) \\ & - \eta_{st\_out}^{-1}\cdot P_{th}^{st,pb}(t_i) - \xi_{st\_loss}\cdot Q_{th}^{st}(t_i)\Big). \end{aligned} \tag{37}$$

As this non-predictive heuristic strategy does not use the knowledge of future developments we just use it as a base-line for the following more advanced strategy.

3.2. Model predictive control using LP formulation

Another option to solve the underlying optimization problem is to use model predictive control as Camacho and Alba (2013, 1990), and to formulate the problem as LP. We use the same temporal discretization as introduced in Section 3.1 with N equidistant time steps, each with a step size of Δt.

At each instance of time t_i for $i = 0,\ldots,N$ we successively regard a sliding time horizon window $[t_i, t_{i+k}]$ for an overall of k future time steps. For the future time steps we assume a precise knowledge of the meteorological parameters as solar irradiation and ambient temperature. For the whole time horizon we want to find optimal assignments for the decision variables, which are the power flows between the concentrated solar block, storage, photovoltaic modules and the grid,

$$u(t_{i+j}|t_i) := \big(P_{th}^{sb,st}(t_{i+j}|t_i),\ P_{th}^{st,pb}(t_{i+j}|t_i),\ P_{th}^{pb}(t_{i+j}|t_i),\ P_{el}^{pv,st}(t_{i+j}|t_i),\ P_{el}^{pv,grid}(t_{i+j}|t_i)\big)^{T}. \tag{38}$$

The expression $P(t_{i+j}|t_i)$ is the power at time t_{i+j}, which was decided at time step t_i. The objective is to maximize the discretized annual revenue R_{annual} (24), which is regarded locally in time for the time horizon window (Vasallo and Bravo, 2016),

$$\max_u \sum_{j=0}^{k}\left(\pi(t_{i+j}|t_i)\cdot\Delta t\cdot\left(\overbrace{\eta_{pb}\big(T_{bulb}(t_{i+j}|t_i)\big)\cdot P_{th}^{pb}(t_{i+j}|t_i)}^{=P_{el}^{pb,grid}(t_{i+j}|t_i)} + P_{el}^{pv,grid}(t_{i+j}|t_i)\right)\right) + \pi^{min}\cdot\eta_{pb}^{min}\cdot Q_{th}^{st}(t_{i+k}|t_i). \tag{39}$$

The additional term rewards the charging of the storage at the end of the time horizon, instead that power is discarded from the system (for the cases when the power block is at full load). We consider the in Section 2 derived constraints on the power flow, express them in dependency of the decision variables u and reformulate them for the discrete forecast window $(t_{i+j}|t_i)$:

- Photovoltaic power flow distribution (1),

$$\underbrace{\eta_{inverter}^{-1}\cdot P_{el}^{pv,grid}(t_{i+j}|t_i)}_{\overset{(3)}{=}P_{el,DC}^{pv,grid}(t_{i+j}|t_i)} + P_{el}^{pv,st}(t_{i+j}|t_i) \leqslant P_{el}^{pv}(t_{i+j}|t_i).$$

- Concentrated solar block power flow distribution (12),

$$\underbrace{P_{th}^{pb}(t_{i+j}|t_i) - P_{th}^{st,pb}(t_{i+j}|t_i)}_{\overset{(18)}{=}P_{th}^{sb,pb}(t_{i+j}|t_i)} + P_{th}^{sb,st}(t_{i+j}|t_i) \leqslant P_{th}^{sb}(t_{i+j}|t_i).$$

- Storage fill level as discretization of the first-order differential Eq. (14),

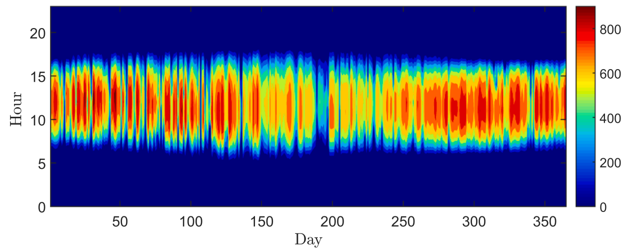

(a) Direct normal irradiation (DNI) I_{DNI} in [W/m^2].

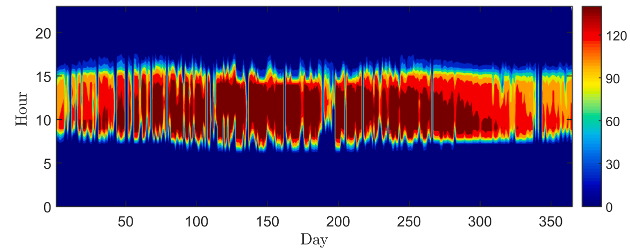

(d) Concentrated solar block thermal output power $P_{\mathrm{th}}^{\mathrm{sb}}$ in [MW$_{\mathrm{th}}$].

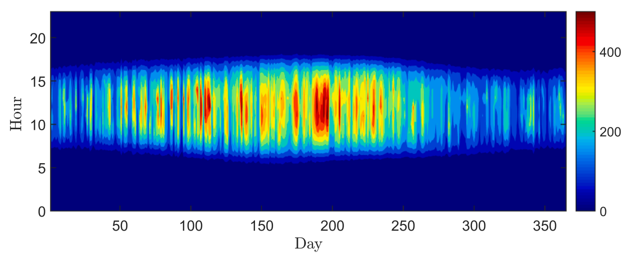

(b) Diffuse horizontal irradiation (DHI) I_{DHI} in [W/m^2].

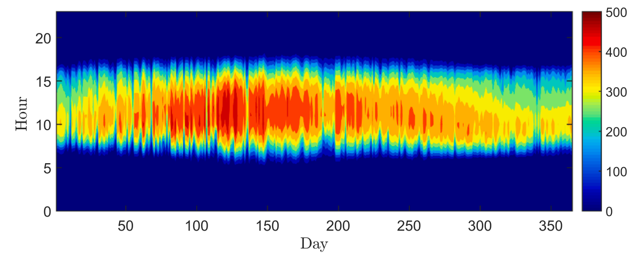

(e) PV electric DC output power $P_{\mathrm{el}}^{\mathrm{pv}}$ in [MW$_{\mathrm{el}}$].

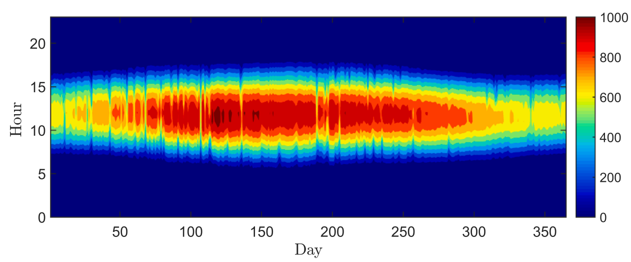

(c) Global horizontal irradiation (GHI) I_{GHI} in [W/m^2].

Fig. 4. Weather data for the reference hybrid CSP-PV power plant at the corresponding site (left), and the resulting CSP and PV power output (right) throughout a year.

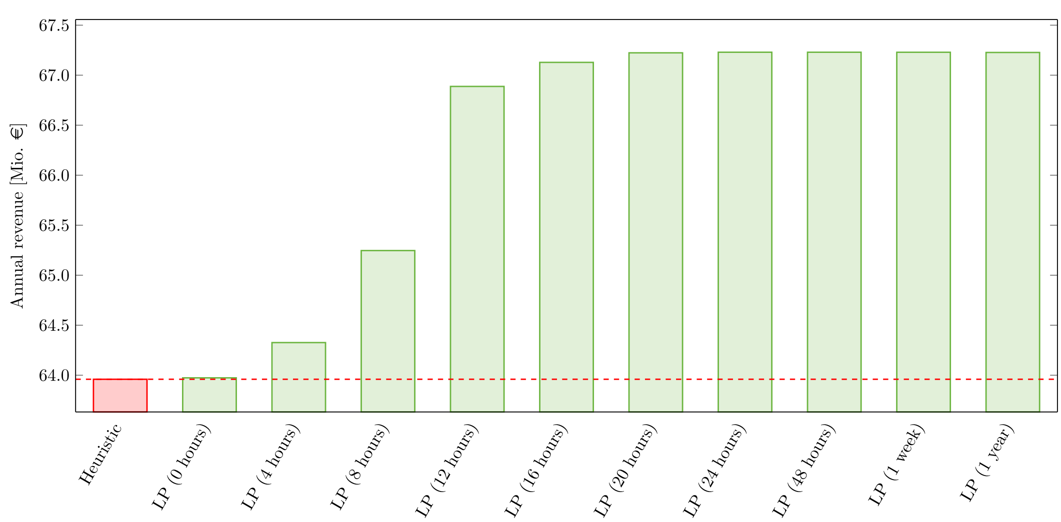

Fig. 5. Annual revenue of the Linear Program in dependency of the time horizon. The reference solution with a time horizon of 8760 h and the solution of the heuristic are indicated as dashed lines.

Table 2
Simulation results of Heuristic and LP storage strategy.

Time horizon	Revenue [Mio. €]	Runtime [sec]
Heuristic	63.96	2.73
0 h	63.97	32.59
4 h	64.33	57.66
8 h	65.25	85.38
12 h	66.89	119.76
16 h	67.13	143.50
20 h	67.22	179.80
24 h	67.23	220.09
28 h	67.23	256.11
32 h	67.23	286.10
36 h	67.23	314.40
40 h	67.23	346.03
44 h	67.23	396.21
48 h	67.23	436.45
168 h	67.23	1278.76
336 h	67.23	2516.71
504 h	67.23	3778.12
672 h	67.23	5030.76
8760 h	67.23	74 715.10

$$Q_{th}^{st}\left(t_{i+j+1}|t_i\right) = Q_{th}^{st}\left(t_{i+j}|t_i\right) + \Delta t\cdot \left(\eta_{st\_in}\cdot P_{th}^{sb,st}\left(t_{i+j}|t_i\right) + \eta_{immersion}\cdot P_{el}^{pv,st}\left(t_{i+j}|t_i\right) - \eta_{st\_out}^{-1}\cdot P_{th}^{st,pb}\left(t_{i+j}|t_i\right) - \xi_{st\_loss}\cdot Q_{th}^{st}\left(t_{i+j}|t_i\right)\right).$$

- Maximum storage capacity (15),

$$0\leqslant Q_{th}^{st}\left(t_{i+j+1}|t_i\right)\leqslant Q_{th}^{st\_max}.$$

- Power block limitations (19),

$$P_{th}^{pb\_min}\leqslant P_{th}^{pb}\left(t_{i+j}|t_i\right)\leqslant P_{th}^{pb\_max}.$$

- Grid energy limitations (22),

$$0\leqslant \underbrace{\eta_{pb}\left(T_{bulb}\left(t_{i+j}|t_i\right)\right)\cdot P_{th}^{pb}\left(t_{i+j}|t_i\right)}_{\overset{(20)}{=}P_{el}^{pb,grid}\left(t_{i+j}|t_i\right)} + P_{el}^{pv,grid}\left(t_{i+j}|t_i\right)\leqslant P_{el}^{max}.$$

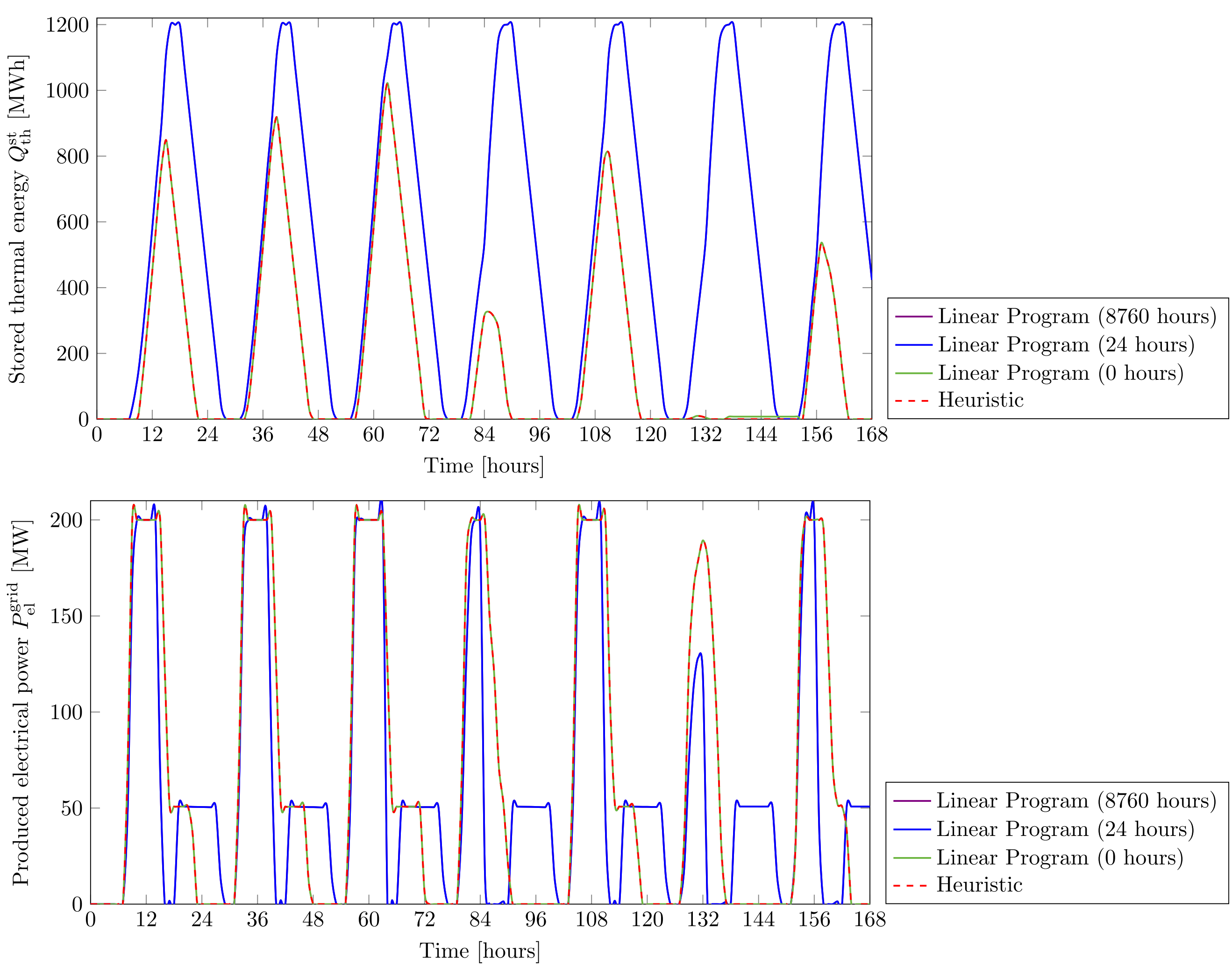

Fig. 6. Storage behavior for the linear program with time frame of 0, 24 and 8760 h. The storage fill level Q_{th}^{st} (above) and the produced electrical power P_{el}^{grid} (below) are plotted for the first 7 days of the year. The LP-24 line (blue) is above the LP-8760 line (violet). (For interpretation of the references to color in this figure legend, the reader is referred to the web version of this article.)

Table 3
Assumed investment and O&M costs of the hybrid CSP-PV power plant. The O&M costs for the hybrid plant are taken from Parrado et al. (2016), Hernández-Moro and Martinez-Duart (2013).

Parameter		Value
i_{rate}	interest rate	3.5 %
ℓ	power plant lifetime	25 years
$c^{\mathrm{sb}}_{\mathrm{invest}}$	Investment costs per concentrated solar block nominal thermal power	570 000 €/MW$_{\mathrm{th}}$
$c^{\mathrm{pb}}_{\mathrm{invest}}$	Investment costs per power block maximum power	240 000 €/MW$_{\mathrm{th}}$
$c^{\mathrm{st}}_{\mathrm{invest}}$	Investment costs per storage maximum capacity	13 000 €/MW$_{\mathrm{th}}$h
$c^{\mathrm{pv}}_{\mathrm{invest}}$	Investment costs per photovoltaic peak power	1 000 000 €/MW$_{\mathrm{el}}$
$f^{\mathrm{sb}}_{\mathrm{O\&M}}$	Operations and maintenance cost factor for concentrated solar block	1.5 %
$f^{\mathrm{pb}}_{\mathrm{O\&M}}$	Operations and maintenance cost factor for power block	1.5 %
$f^{\mathrm{st}}_{\mathrm{O\&M}}$	Operations and maintenance cost factor for storage	1.5 %
$f^{\mathrm{pv}}_{\mathrm{O\&M}}$	Operations and maintenance cost factor for photovoltaic modules	1.5 %

The storage fill level at t_0 is given as boundary condition, as defined in (17),

$$Q^{\mathrm{st}}_{\mathrm{th}}\left(t_0|t_0\right) := 0, \tag{40}$$

As further boundary conditions, at each instance of time the power flows from the concentrated solar block $P^{\mathrm{sb}}_{\mathrm{th}}$ and photovoltaic cells $P^{\mathrm{pv}}_{\mathrm{el}}$, the tariff π, and the bulb temperature T_{bulb} (needed by the power block) are given. Thus, successively at each instance of time t_i with a sliding time horizon window the five control parameters $u(t_i)$ needs to be decided in such a way that the above formulated constraints are satisfied

With the simplified assumption in (21) that the power block efficiency η_{pb} is not dependent on the thermal power flow $P^{\mathrm{pb}}_{\mathrm{th}}$, the underlying optimization problem has a linear objective function and linear constraints. In such a way the developed linear optimization problem can be solved with a LP solver, as e.g. Gurobi (Gu et al., 2012).

4. Case study

In this section we present the results for a sample power plant. To test the storage strategies a realistic scenario for a location in the MENA[2] region is drawn. All parameter of the reference power plant settings are summarized in Table 1. For meteorological data, the EnergyPlus[3] database for Casablanca in Morocco is used, which lists all needed parameters as wind speed, pressure, temperature and solar irradiation for a full year on an hourly resolution. In Figs. 4 (a), (b) and (c) the annual solar irradiation for $I_{\mathrm{DNI}}, I_{\mathrm{DHI}}$ and I_{GHI} are visualized. For the given meteorological data and the introduced reference hybrid CSP-PV power plant, the thermal power $P^{\mathrm{sb}}_{\mathrm{th}}$ of the CSP plant and electric power from the PV plant $P^{\mathrm{pv}}_{\mathrm{el}}$ are visualized in Figs. 4 (d) and (e).

4.1. Storage strategies for different tariffs

The meteorological data bases on hourly data of a full year (8760 h). To avoid that the time horizon of the Linear Program exceeds the length of the meteorological data set while simulating the first 8760 h, we consecutively use two times the same data set with a total length of 17520 h

The quality of the reached annual revenue from Eq. (24) for the LP depends on the time horizon, see Fig. 5. As reference, the annual revenue of the LP with a time horizon of 8760 h in a year is used which has an annual revenue of 67.23 Mio. €. The weakest solution of the LP has a time horizon of 0 h with an annual revenue of 63.97 Mio. €. In comparison, the annual revenue of the heuristic delivers 63.96 Mio. € which corresponds to 95.2 % of the reference solution (LP-8760). The results are summarized in Table 2.

Based on these results a time horizon of 24 h is recommended, as with this choice a large revenue at low run-time can be reached. Consider that the LP scheduler assumes a precise knowledge of the future meteorological parameters as solar irradiation and ambient temperature. Thus, the here-in shown results should be seen as upper bound for the time horizon, as with noisy meteorological data the quality of long time horizons would not be that beneficial.

The behavior of the storage strategies is shown in Fig. 6, where the storage fill level $Q^{\mathrm{st}}_{\mathrm{th}}$ and the produced electrical power $P^{\mathrm{grid}}_{\mathrm{el}}$ are shown. It can be seen, the larger the time horizon of the LP, the more the solution converges to the reference solution. While the other way around, the smaller the time horizon of the LP, the more the solution converges to the heuristic.

The LP solution with a **time horizon of 24 h** reaches an annual revenue of 67.23 Mio. €, which corresponds to the value of the reference solution of LP-8760. We choose this time horizon for the following investigations, as the runtime is low and the reached annual revenue is already close to the reference value. As the prediction of meteorological data for more than 24 h gets more and more uncertain, a larger time frame seems not to be convenient without considering uncertainties of the underlying meteorological forecast model.

4.2. Optimal layout of a hybrid CSP-PV power plant

The layout of a power plant can be measured by different economic quantities. In the following we present the annual gain rate and the net present value:

- The *annual gain rate* takes into account the annual revenue R_{annual} (23) and its total investment costs (downscaled to one year),

$$i_{\mathrm{gain}} = \frac{R_{\mathrm{annual}} - C_{\mathrm{invest}} \cdot f_{\mathrm{annuity}} - C_{\mathrm{O\&M}}}{C_{\mathrm{invest}} \cdot f_{\mathrm{annuity}} + C_{\mathrm{O\&M}}}, \tag{41}$$

with annuity factor $f_{\mathrm{annuity}} := \frac{(1+i_{\mathrm{rate}})^{\ell} \cdot i_{\mathrm{rate}}}{(1+i_{\mathrm{rate}})^{\ell} - 1}$, interest rate i_{rate}, and the plant lifetime of ℓ years. The investment costs C_{invest} of a CSP-PV hybrid power plant are computed in dependency of the size or capacity of each component,

$$C_{\mathrm{invest}} := \underbrace{c^{\mathrm{sb}}_{\mathrm{invest}} \cdot P^{\mathrm{sb-nominal}}_{\mathrm{th}}}_{C^{\mathrm{sb}}_{\mathrm{invest}}} + \underbrace{c^{\mathrm{pb}}_{\mathrm{invest}} \cdot P^{\mathrm{pb-max}}_{\mathrm{th}}}_{C^{\mathrm{pb}}_{\mathrm{invest}}} + \underbrace{c^{\mathrm{st}}_{\mathrm{invest}} \cdot Q^{\mathrm{st-max}}_{\mathrm{th}}}_{C^{\mathrm{st}}_{\mathrm{invest}}} + \underbrace{c^{\mathrm{pv}}_{\mathrm{invest}} \cdot P^{\mathrm{pv-peak}}_{\mathrm{el}}}_{=:C^{\mathrm{pv}}_{\mathrm{invest}}}, \tag{42}$$

while the annual operation and maintenance costs $C_{\mathrm{O\&M}}$ are given as factor of these investment costs,

[2] Middle East and North Africa.
[3] EnergyPlus weather file https://energyplus.net/weather.

Table 4
Resulting annual revenue (in Mio. €) using the heuristic across the steps of a multidimensional Newton-Raphson method for layout optimization.

Step	$Q_{th}^{st\_max}$	$P_{th}^{sb\_nominal}$	$P_{th}^{pb\_max}$	$P_{el}^{pv\_peak}$	R_{annual}
0	1500 $\mathrm{MW_{th}h}$	150 $\mathrm{MW_{th}}$	125 $\mathrm{MW_{th}}$	396.1 $\mathrm{MW_{el}}$	67.163 Mio. €
1	1500 $\mathrm{MW_{th}h}$	200 $\mathrm{MW_{th}}$	125 $\mathrm{MW_{th}}$	367.6 $\mathrm{MW_{el}}$	67.792 Mio. €
2	2000 $\mathrm{MW_{th}h}$	200 $\mathrm{MW_{th}}$	125 $\mathrm{MW_{th}}$	361.1 $\mathrm{MW_{el}}$	69.975 Mio. €
3	2000 $\mathrm{MW_{th}h}$	200 $\mathrm{MW_{th}}$	150 $\mathrm{MW_{th}}$	355.1 $\mathrm{MW_{el}}$	70.784 Mio. €
4	2000 $\mathrm{MW_{th}h}$	250 $\mathrm{MW_{th}}$	150 $\mathrm{MW_{th}}$	326.6 $\mathrm{MW_{el}}$	71.401 Mio. €
5	2500 $\mathrm{MW_{th}h}$	250 $\mathrm{MW_{th}}$	150 $\mathrm{MW_{th}}$	320.1 $\mathrm{MW_{el}}$	72.200 Mio. €
6	2500 $\mathrm{MW_{th}h}$	300 $\mathrm{MW_{th}}$	150 $\mathrm{MW_{th}}$	291.6 $\mathrm{MW_{el}}$	72.732 Mio. €
7	2500 $\mathrm{MW_{th}h}$	300 $\mathrm{MW_{th}}$	175 $\mathrm{MW_{th}}$	285.6 $\mathrm{MW_{el}}$	73.081 Mio. €
8	2500 $\mathrm{MW_{th}h}$	350 $\mathrm{MW_{th}}$	175 $\mathrm{MW_{th}}$	257.1 $\mathrm{MW_{el}}$	73.317 Mio. €

Table 5
Resulting annual revenue (in Mio. €) using the LP with a time horizon of 24 h across the steps of a multidimensional Newton-Raphson method for layout optimization.

Step	$Q_{th}^{st\_max}$	$P_{th}^{sb\_nominal}$	$P_{th}^{pb\_max}$	$P_{el}^{pv\_peak}$	R_{annual}
0	1500 $\mathrm{MW_{th}h}$	150 $\mathrm{MW_{th}}$	125 $\mathrm{MW_{th}}$	396.1 $\mathrm{MW_{el}}$	70.023 Mio. €
1	1500 $\mathrm{MW_{th}h}$	200 $\mathrm{MW_{th}}$	125 $\mathrm{MW_{th}}$	367.6 $\mathrm{MW_{el}}$	70.659 Mio. €
2	1500 $\mathrm{MW_{th}h}$	200 $\mathrm{MW_{th}}$	150 $\mathrm{MW_{th}}$	361.6 $\mathrm{MW_{el}}$	71.454 Mio. €
3	2000 $\mathrm{MW_{th}h}$	200 $\mathrm{MW_{th}}$	150 $\mathrm{MW_{th}}$	355.1 $\mathrm{MW_{el}}$	74.731 Mio. €
4	2000 $\mathrm{MW_{th}h}$	200 $\mathrm{MW_{th}}$	175 $\mathrm{MW_{th}}$	349.1 $\mathrm{MW_{el}}$	75.430 Mio. €
5	2000 $\mathrm{MW_{th}h}$	200 $\mathrm{MW_{th}}$	200 $\mathrm{MW_{th}}$	343.1 $\mathrm{MW_{el}}$	75.698 Mio. €
6	2000 $\mathrm{MW_{th}h}$	250 $\mathrm{MW_{th}}$	200 $\mathrm{MW_{th}}$	314.6 $\mathrm{MW_{el}}$	76.691 Mio. €
7	2000 $\mathrm{MW_{th}h}$	300 $\mathrm{MW_{th}}$	200 $\mathrm{MW_{th}}$	286.1 $\mathrm{MW_{el}}$	77.317 Mio. €
8	2500 $\mathrm{MW_{th}h}$	300 $\mathrm{MW_{th}}$	200 $\mathrm{MW_{th}}$	279.6 $\mathrm{MW_{el}}$	79.663 Mio. €
9	3000 $\mathrm{MW_{th}h}$	300 $\mathrm{MW_{th}}$	200 $\mathrm{MW_{th}}$	273.1 $\mathrm{MW_{el}}$	80.179 Mio. €
10	3000 $\mathrm{MW_{th}h}$	350 $\mathrm{MW_{th}}$	200 $\mathrm{MW_{th}}$	244.6 $\mathrm{MW_{el}}$	81.130 Mio. €
11	3000 $\mathrm{MW_{th}h}$	350 $\mathrm{MW_{th}}$	225 $\mathrm{MW_{th}}$	238.6 $\mathrm{MW_{el}}$	81.652 Mio. €
12	3000 $\mathrm{MW_{th}h}$	400 $\mathrm{MW_{th}}$	225 $\mathrm{MW_{th}}$	210.1 $\mathrm{MW_{el}}$	82.414 Mio. €
13	3000 $\mathrm{MW_{th}h}$	450 $\mathrm{MW_{th}}$	225 $\mathrm{MW_{th}}$	181.6 $\mathrm{MW_{el}}$	82.786 Mio. €
14	3000 $\mathrm{MW_{th}h}$	450 $\mathrm{MW_{th}}$	250 $\mathrm{MW_{th}}$	175.6 $\mathrm{MW_{el}}$	83.306 Mio. €
15	3000 $\mathrm{MW_{th}h}$	450 $\mathrm{MW_{th}}$	275 $\mathrm{MW_{th}}$	169.6 $\mathrm{MW_{el}}$	83.658 Mio. €

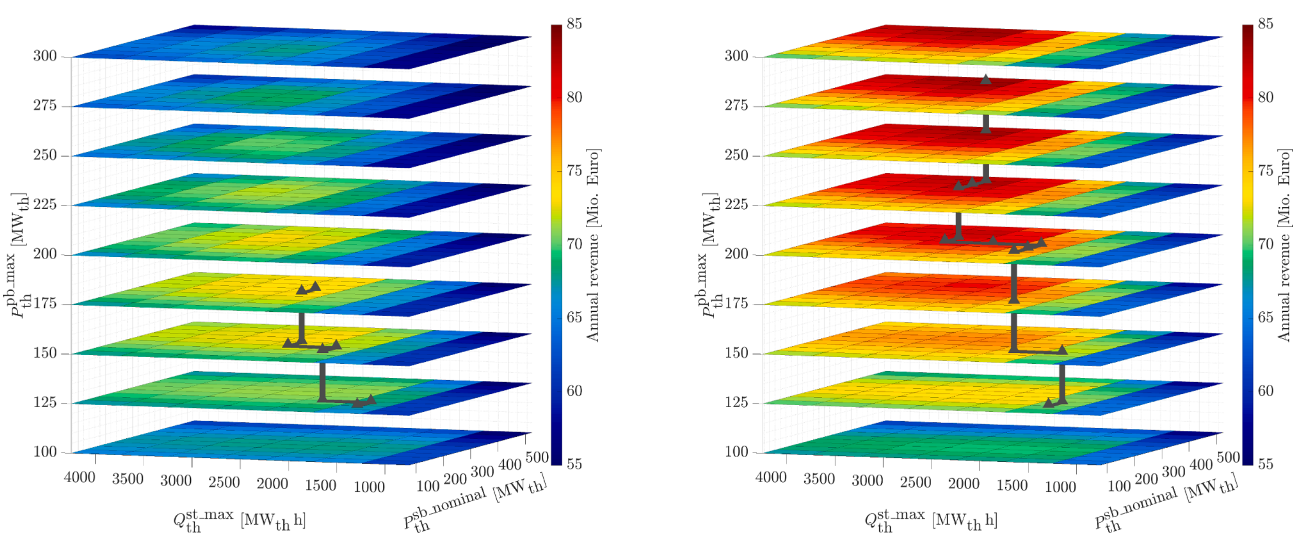

(a) Heuristic

(b) LP with a time horizon of 24 hours

Fig. 7. Resulting annual revenue (in Mio. €) using the heuristic (left) and the LP with a time horizon of 24 h (right), for different scenarios for storage capacity, concentrated solar block size, powerblock size and resulting photovoltaic size.

Table 6
Best simulation results using the heuristic and the LP storage strategy with a time horizon of 24 h.

		Reference configuration	Optimized configuration using heuristic	Optimized configuration using LP (24 hours)
$P_{th}^{sb\_nominal}$	Concentrated solar block nominal thermal power	150 MW_{th}	350 MW_{th}	450 MW_{th}
$P_{th}^{pb\_max}$	Power block maximum power	125 MW_{th}	175 MW_{th}	275 MW_{th}
$Q_{th}^{st\_max}$	Storage maximum capacity	1200 $MW_{th}h$	2500 $MW_{th}h$	3000 $MW_{th}h$
$P_{el}^{pv\_peak}$	Photovoltaic peak power	400 MW_{el}	257.1 MW_{el}	169.6 MW_{el}
C_{invest}^{sb}	Investment costs for concentrated solar block	85.5 Mio. €	199.5 Mio. €	256.5 Mio. €
C_{invest}^{pb}	Investment costs for power block	30.0 Mio. €	42.0 Mio. €	66.0 Mio. €
C_{invest}^{st}	Investment costs for storage	15.6 Mio. €	32.5 Mio. €	39.0 Mio. €
C_{invest}^{pv}	Investment costs for PV	400 Mio. €	257.1 Mio. €	169.6 Mio. €
C_{invest}	Total investment costs	531.1 Mio. €	531.1 Mio. €	531.1 Mio. €
R_{annual}	Annual revenue	63.96 Mio. €	73.3 Mio. €	83.7 Mio. €
i_{gain}	Annual gain rate	0.59 %	0.93 %	1.34 %
C_{NPV}	Net present value	391.8 Mio. €	582.0 Mio. €	790.1 Mio. €

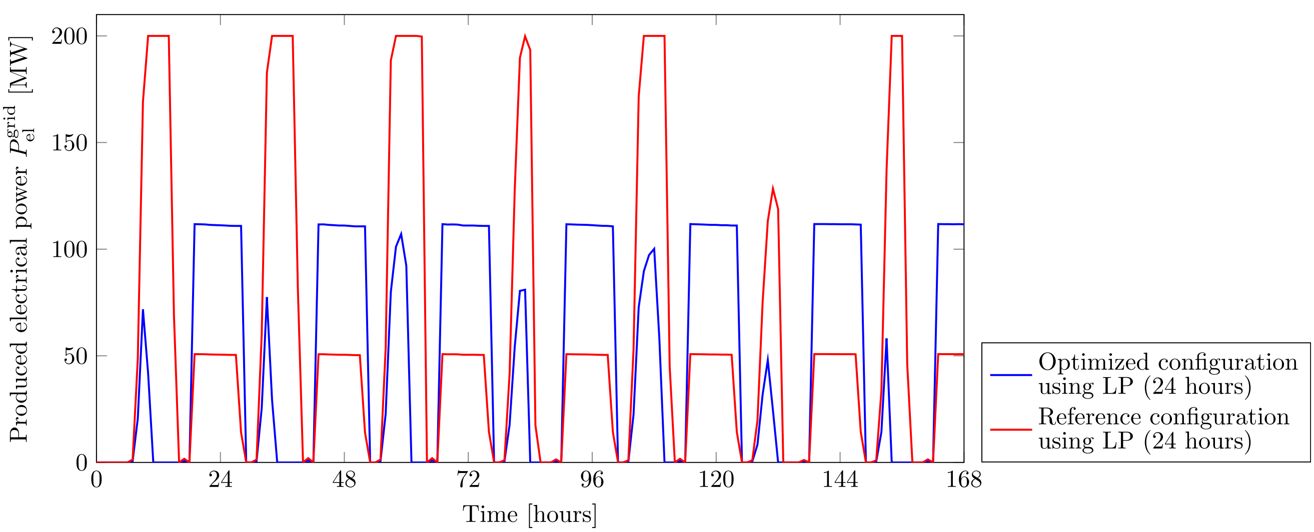

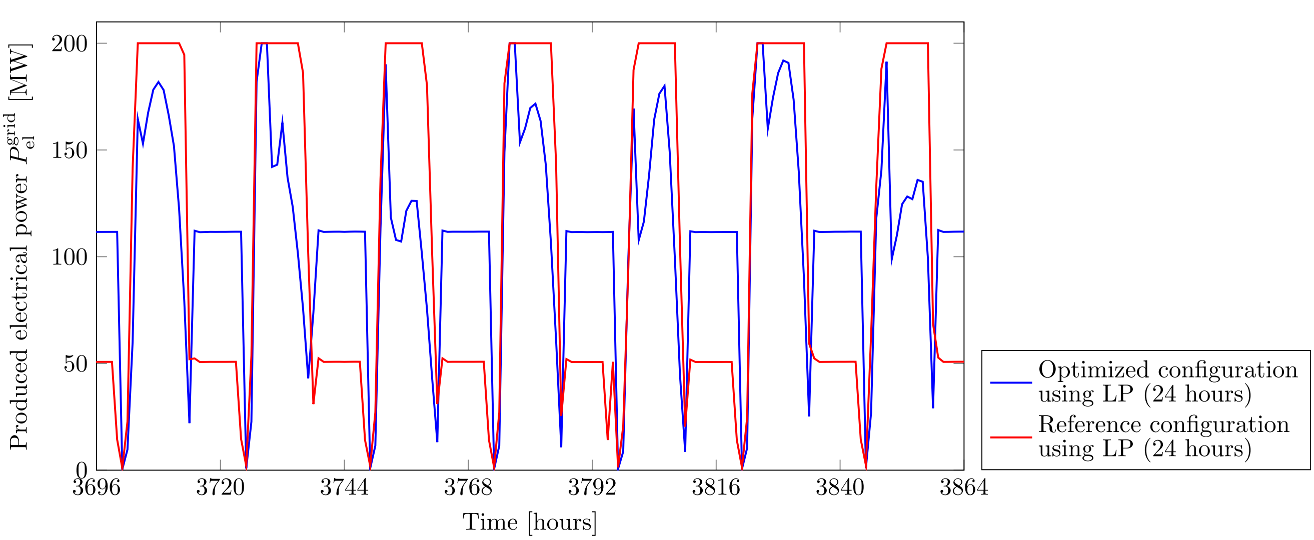

Fig. 8. Electrial power production P_{el}^{grid} for the optimized configuration and reference configuration, both using LP (24 h), during a winter (above) and summer (below) week.

$$C_{\mathrm{O\&M}} := C^{\mathrm{sb}}_{\mathrm{invest}} \cdot f^{\mathrm{sb}}_{\mathrm{O\&M}} + C^{\mathrm{pb}}_{\mathrm{invest}} \cdot f^{\mathrm{pb}}_{\mathrm{O\&M}} + C^{\mathrm{st}}_{\mathrm{invest}} \cdot f^{\mathrm{st}}_{\mathrm{O\&M}} + C^{\mathrm{pv}}_{\mathrm{invest}} \cdot f^{\mathrm{pv}}_{\mathrm{O\&M}}. \quad (43)$$

- The *net present value* (González et al., 2009) represents the sum of all investments and values of all incomes and expenses over the project lifetime, which is the incomes and expenses of each year, while considering the interest rate (Augsburger, 2013; Heiming, 2017),

$$C_{\mathrm{NPV}} = \sum_{t=1}^{\ell} \frac{R_{\mathrm{annual}} - C_{\mathrm{O\&M}}}{(1 + i_{\mathrm{rate}})^t} - C_{\mathrm{invest}}. \quad (44)$$

In Table 3 values are given for all these costs. Thus, for the reference power plant, the investment costs of the PV plant amounts to 400 Mio. €, the solar field to 85.5 Mio. €, the storage cost to 15.6 Mio. €, and the power block to 30 Mio. €, which sum to a total of

$$C^{\mathrm{reference}}_{\mathrm{invest}} := 531.1\mathrm{M}€. \quad (45)$$

In the following we investigate the quality of the reference power plant according to the chosen power block maximum power for operation $P^{\mathrm{pb-max}}_{\mathrm{th}}$, the storage capacity $Q^{\mathrm{st-max}}_{\mathrm{th}}$ and the nominal thermal power of the CSP plant $P^{\mathrm{sb-nominal}}_{\mathrm{th}}$, while choosing the peak power of the photovoltaic modules $P^{\mathrm{pv-peak}}_{\mathrm{el}}$ such that the total investment costs $C_{\mathrm{invest}} \stackrel{!}{=} C^{\mathrm{reference}}_{\mathrm{invest}}$ are for all cases equal. We confine the search space to a set of realistic values, such that $Q^{\mathrm{st-max}}_{\mathrm{th}} \leqslant 4000$ $\mathrm{MW_{th}h}$, $P^{\mathrm{sb-nominal}}_{\mathrm{th}} \leqslant 500$ $\mathrm{MW_{th}}$ and $P^{\mathrm{pb-max}}_{\mathrm{th}} \leqslant 300$ $\mathrm{MW_{th}}$.

As the total investment costs for all cases stay constant we here just regard the annual revenue. For a fast optimization a multidimensional Newton-Raphson method can be used (Deuflhard, 2011). The search space is defined by three dimensions (adjustable parameters) to which we apply the secant method independently to obtain numerically approximated gradients for the Newton-Raphson method.

In Tables 4 and 5 the resulting annual revenue using the heuristic and the LP with a time horizon of 24 h are shown for the steps of the Newton-Raphson method. A visualization of the resulting annual revenue for each scenario within the search space is given in Fig. 7, where the *optimization path* of the Newton-Raphson method is drawn as a black line. It can be seen that for each configuration the heuristic strategy always delivers worse results than the LP strategy. We should emphasize that the outcome of the configuration optimization strongly depends on the feed-in-tariff $\pi(t)$ which varies with a factor of 2.9 between high and low tariff, see Table 1.

Furthermore, both strategies reach two different optima for the configuration, see Table 6. The LP with a time horizon of 24 h reaches its optimum for a larger maximum power block power $P^{\mathrm{pb-max}}_{\mathrm{th}}$ of 275 $\mathrm{MW_{th}}$ (compared to 175 $\mathrm{MW_{th}}$ for the heuristic), and a larger concentrated solar block $P^{\mathrm{sb-nominal}}_{\mathrm{th}}$ of 450 $\mathrm{MW_{th}}$ (compared to 350 $\mathrm{MW_{th}}$ for the heuristic). On the other hand, the LP maxed out for a smaller PV field $P^{\mathrm{pv-peak}}_{\mathrm{el}}$ of 169.6 $\mathrm{MW_{el}}$ (compared to 257.1 $\mathrm{MW_{el}}$ for the heuristic). Interstingly, both strategies deliver comparable storage capacities $Q^{\mathrm{st-max}}_{\mathrm{th}}$ of 3000 $\mathrm{MW_{th}h}$ for the LP and 2500 $\mathrm{MW_{th}h}$ for the heuristic. The optimal configuration of the LP delivers an annual revenue R_{annual} of 83.7 Mio. €, compared to 73.3 Mio. € for the heuristic, which is a gain of 14.2 %. Compared to the reference power plant the gain is 24.4 %. It is interesting to see that the operation strategy has such a large influence on the optimal design of the power plant.

To analyze why the optimum for the LP storage strategy is reached with this specific setup, Fig. 8 compares the electrial power production of this optimized power plant with that of the reference power plant during a winter and summer week. We find that the larger storage capacity $Q^{\mathrm{st-max}}_{\mathrm{th}}$ paired with the higher power block maximum power $P^{\mathrm{pb-max}}_{\mathrm{th}}$ allows to minimize the excess power during daytime, instead storing it to produce more electrical power at night time. As described in Section 2, the turbine of the powerblock can only operate within in a certain range (19). This means during night the production of electrical power $P^{\mathrm{grid}}_{\mathrm{el}}$ is limited to roughly 50 $\mathrm{MW_{th}}$ for the reference power plant, while the optimized plant is able to produce electrical power in excess of 100 $\mathrm{MW_{th}}$ at this time. The increased concentrated solar block nominal thermal power $P^{\mathrm{sb-nominal}}_{\mathrm{th}}$ allows to store more power during day. The in turn lower investment in photovoltaic and higher storage activity is visible, as the optimized power plant regularly produces less electrical power during daytime, especially in winter. However, the advantage of higher electrical power production $P^{\mathrm{grid}}_{\mathrm{el}}$ at night, where the tariff is higher, far outweighs this disadvantage.

4.3. Discussion of the results

For a hybrid CSP-PV power plant a LP storage strategy with a time horizon of 24 h yields already the same results as using larger time horizons, see Table 2. Even with a time horizon of 0 h, the LP storage strategy slightly outperforms the heuristic. Hence, the LP storage strategy should clearly be preferred. As the calculation of a full year, using this LP storage strategy with time horizon of 24 h, takes only a few hundred seconds on a standard computer, see Table 2, we can calculate a single time step (e.g. one hour) in less than a second. Thus, this strategy can also be used for real-time control.

For the layout optimization of a hybrid CSP-PV power plant, the optimal configuration differs significantly depending on the used storage strategy, see Table 6. The optimized power plant with LP storage strategy yields a 14.2 % higher annual revenue compared to the optimized power plant with heuristic storage strategy. Therefore it is strongly recommendable to use the LP storage strategy especially for layout optimization.

5. Conclusion

In this work a new real-time storage strategy using model predictive control is developed for a hybrid CSP-PV plant. This type of hybrid solar power plant makes use of both the cheap thermal storage system of CSP and the cheap electricity production of PV. The future energy tariff and future weather conditions are factored into a Linear Program storage strategy. Different time horizons for this LP storage strategy are investigated and compared to a non-predictive heuristic storage strategy. Both strategies consider the efficiency of the power block as quadratic function depending on the bulb temperature. In a case study it is shown that using this LP storage strategy with a time horizon of 24 h yields already the same annual revenue as using larger time horizons.

For layout optimization of the hybrid CSP-PV power plant the optimal configuration differs significantly depending on the used storage strategy. It is shown that the optimal configuration of the LP storage strategy is 14.2 % better than using a non-predictive heuristic storage strategy.

Altogether, for the operation of a hybrid CSP-PV power plant the usage of a LP storage strategy is highly recommended as this exact optimizer delivers a global optimum within a reasonable period. Furthermore, the LP storage strategy should also be used for the layout optimization, as the impact of the storage strategy on the final configuration is large.

Future work. The current work only considers the upper limit on the power that can be released to the grid. The work can be extended by adding a lower limit on the power that can be released at different times of the day. Furthermore, the temperature-dependent power block efficiency should also be dependent on the thermal load, which will cause a non-linear optimization problem. So far, the storage model neglects heating-up times for the thermal storage. In future this constraint should be considered as it has an effect on the annual energy production. For the photovoltaic model, the capacity size of the PV inverter should be considered (and optimized) independently from the nominal capacity of the PV modules. For the power block the turbine efficiency should also consider the thermal load. In order to keep the linear property of the formulated optimization problem, a discretized step function can be used.

Declaration of Competing Interest

The authors declare that they have no known competing financial interests or personal relationships that could have appeared to influence the work reported in this paper.

Acknowledgments

The authors thank Stella Coumbassa for her help to code the formulated linear problem.

References

Ahlbrink, N., Belhomme, B., Flesch, R., Maldonado Quinto, D., Rong, A., Schwarzbözl, P., 2012. Stral: Fast ray tracing software with tool coupling capabilities for high-precision simulations of solar thermal power plants. In: Proceedings of the SolarPACES 2012 conference, p. 1.
Augsburger, G., 2013. Thermo-economic optimisation of large solar tower power plants (PhD thesis). École Polytechnique Fédérale de Lausanne.
Camacho, E.F., Alba, C.B., 2013. Model predictive control. Springer Science & Business Media.
Camacho, E.F., Berenguel, M., 2012. Control of solar energy systems. IFAC Proc. Vol. 45 (15), 848–855.
Camacho, E.F., Gallego, A.J., 2015. Model predictive control in solar trough plants: a review. IFAC-PapersOnLine 48 (23), 278–285.
Camacho, E.F., Berenguel, M., Gallego, A.J., 2014. Control of thermal solar energy plants. J. Process Control 24 (2), 332–340.
Casella, F., Casati, E., Colonna, P., 2014. Optimal operation of solar tower plants with thermal storage for system design. IFAC Proc. Vol. 47 (3), 4972–4978.
Cirocco, L.R., Belusko, M., Bruno, F., Boland, J., Pudney, P., 2015. Controlling stored energy in a concentrating solar thermal power plant to maximise revenue. IET Renew. Power Gener. 9 (4), 379–388.
Cirocco, L.R., Belusko, M., Bruno, F., Boland, J., Pudney, P., 2016. Maximising revenue via optimal control of a concentrating solar thermal power plant with limited storage capacity. IET Renew. Power Gener. 10 (5), 729–734.
Deuflhard, P., 2011. Newton methods for nonlinear problems: affine invariance and adaptive algorithms, vol. 35. Springer Science & Business Media.
Dominio, F., 2014. Techno-economic analysis of hybrid PV-CSP power plants. Advantages and disadvantages of intermediate and peak load operation (Master's thesis). Universitat Politècnica de Catalunya.
Duffie, J.A., Beckman, W.A., 2013. Solar engineering of thermal processes. John Wiley & Sons.
González, J.S., Rodríguez, A.G., Mora, J.C., Santos, J.R., Payán, M.B., 2009. A new tool for wind farm optimal design. In: PowerTech, 2009 IEEE Bucharest. IEEE, pp. 1–7.
Gu, Z., Rothberg, E., Bixby, R., 2012. Gurobi optimizer reference manual, version 5.0. Technical report. Gurobi Optimization Inc., Houston, USA.
Guédez, J., Spelling, R., Laumert, B., Fransson, T., 2014. Optimization of thermal energy storage integration strategies for peak power production by concentrating solar power plants. Energy Procedia 49, 1642–1651.
Heiming, G., 2017. Development of a techno-economic model for solar tower power plants (Master's thesis). RWTH Aachen University.
Hernández-Moro, J., Martinez-Duart, J.M., 2013. Analytical model for solar pv and CSP electricity costs: Present LCOE values and their future evolution. Renew. Sustain. Energy Rev. 20, 119–132.
Masters, G.M., 2013. Renewable and efficient electric power systems. John Wiley & Sons.
Mayne, D.Q., Michalska, H., 1990. Receding horizon control of nonlinear systems. IEEE Trans. Automatic Control 35 (7), 814–824.
Parida, B., Iniyan, S., Goic, R., 2011. A review of solar photovoltaic technologies. Renew. Sustain. Energy Rev. 15 (3), 1625–1636.
Parrado, C., Girard, A., Simon, F., Fuentealba, E., 2016. 2050 lcoe (levelized cost of energy) projection for a hybrid PV (photovoltaic)-CSP (concentrated solar power) plant in the atacama desert, chile. Energy 94, 422–430.
Usaola, J., 2012. Operation of concentrating solar power plants with storage in spot electricity markets. IET Renew. Power Gener. 6 (1), 59–66.
Vasallo, M.J., Bravo, J.M., 2016. A MPC approach for optimal generation scheduling in CSP plants. Appl. Energy 165, 357–370.
Wittmann, M., Eck, M., Pitz-Paal, R., Müller-Steinhagen, H., 2011. Methodology for optimized operation strategies of solar thermal power plants with integrated heat storage. Sol. Energy 85 (4), 653–659.
Zhai, R., Chen, Y., Liu, H., Wu, H., Yang, Y., 2018. Optimal design method of a hybrid CSP-PV plant based on genetic algorithm considering the operation strategy. Int. J. Photoenergy 2018.